ROYAL SOCIETY
OF CHEMISTRY

Check for updates

The degree of electron itinerancy and shell closing in the core-ionized state of transition metals probed by Auger-photoelectron coincidence spectroscopy†

Artur Born,‡[abc] Fredrik O. L. Johansson, [ID] ‡*[de] Torsten Leitner,[ab] Ieva Bidermane,[ab] Danilo Kühn,[ab] Nils Mårtensson[af] and Alexander Föhlisch [ID] *[abc]

Auger-photoelectron coincidence spectroscopy (APECS) has been used to examine the electron correlation and itinerance effects in transition metals Cu, Ni and Co. It is shown that the LVV Auger, in coincidence with 2p photoelectrons, spectra can be represented using atomic multiplet positions if the 3d-shell is localized (atomic-like) and with a self-convoluted valence band for band-like (itinerant) materials as explained using the Cini–Sawatzky model. For transition metals, the 3d band changes from band-like to localized with increasing atomic number, with the possibility of a mixed behavior. Our result shows that the LVV spectra of Cu can be represented by atomic multiplet calculations, those of Co resemble the self-convolution of the valence band and those of Ni are a mixture of both, consistent with the Cini–Sawatzky model.

1 Introduction

The necessity for small and still powerful electronic devices requires a deeper understanding of physical effects especially those affecting the electronic properties of solid state materials. In particular, 3d metals are among the most widely used materials for engineering purposes.[1–5] 3d metals and their alloys cover a wide range of electronic properties such as semiconductivity (Cu$_2$O), superconductivity (cuprates) or metal to insulator transitions in *e.g.* Fe$_3$O$_4$ and also magnetic properties such as antiferromagnetism in NiO or ferromagnetism in pure Ni, Co and Fe. This is due to the very sensitive electronic structure of 3d metals to the chemical environment and stoichiometry.[6–8]

X-Ray photoelectron spectroscopy (XPS) and Auger electron spectroscopy (AES) have become established tools for probing the electronic structure, the chemical environment or even dynamic effects. Specifically, AES is well suited to study the electron correlation effects, since it is sensitive to the two-hole states. In practice, however, the fact that the initial ionization and the Auger decay are closely correlated is usually ignored leading to challenging interpretation of the data within simplistic models. In XPS or AES already the pure metals exhibit overlapping and indistinguishable spectral shapes[9,10] and strong satellites,[9,11,12] due to correlation effects, multiplet splittings, screening effects, shake-up processes or Coster–Kronig (CK) decay and also due to a mixed ground state configuration. Thus, true interpretation of electron spectra can be particularly difficult.

Auger-photoelectron coincidence spectroscopy (APECS) explicitly uses the correlation between the photoelectron and the Auger electron, which enables the separation of spectral features and allows for a clear assignment. This is due to the simultaneous measurement of the photoelectron and the, during the core-hole decay produced, Auger electron. Within this measurement scheme it can be ensured that both electrons originate from the same site and ionization event. Therefore, every data point contains information about the initial photoionization and the subsequent relaxations. In this paper APECS

[a] Uppsala-Berlin Joint Laboratory on Next Generation Photoelectron Spectroscopy, Albert-Einstein-Str. 15, 12489, Berlin, Germany.
E-mail: alexander.foehlisch@helmholtz-berlin.de
[b] Institute for Methods and Instrumentation in Synchrotron Radiation Research FG-ISRR, Helmholtz-Zentrum Berlin für Materialien und Energie Albert-Einstein-Strasse 15, 12489, Berlin, Germany
[c] Institut für Physik und Astronomie, Universität Potsdam, Karl-Liebknecht-Strasse 24-25, 14476, Potsdam, Germany
[d] Division of Applied Physical Chemistry, Department of Chemistry, KTH – Royal Institute of Technology, SE-100 44, Stockholm, Sweden. E-mail: fjson@kth.se
[e] Sorbonne Université, CNRS, Institut des NanoSciences de Paris, INSP, F-75005, Paris, France
[f] Department of Physics and Astronomy, Division of X-ray Photon Science, Uppsala University, P. O. Box 256, SE-751 05, Uppsala, Sweden
† Electronic supplementary information (ESI) available: Providing a detailed description of the data acquisition and treatment. See DOI: **https://doi.org/10.1039/d2cp02477b**
‡ These authors contributed equally to this work.

is used to study the $L_{2,3}VV$ Auger decay in Cu, Ni and Co originating in specifically selected core-excites states.

The LVV Auger spectra were explained by Cini and Sawatzky[13–16] using atomic multiplet positions when the 3d-shell is localized but for band-like materials the LVV spectra instead resemble the self-convoluted valence band. For transition metals, the 3d band changes from band-like or itinerant to atomic-like or localized with increasing atomic number, where also a mixed situation is possible as in Ni. As was shown by Haak et al.[17] the Cu $L_{2,3}VV$ Auger spectra can be represented by atomic multiplet calculations and as later shown by Sawatzky[18] they also contain a small bandlike contribution at higher kinetic energies as predicted by Cini–Sawatzky theory but at energies falling outside the measurement region of this study. From its energy band structure it is seen that this weak contribution is dominated by the 3d band. It is also seen that the contribution to the Auger spectrum involving the 4sp states is negligible. As we have shown for Ni[19] one needs to use the self-convolution of the valence band in addition to the atomic multiplet calculations in order to represent the mixed nature of the $L_{2,3}VV$ spectra. Co on the other hand, behaves as an itinerant metal and the spectrum resembles the self-convolution of the valence band. Notably, Lund et al.[10] found that the L_3VV and the L_2VV CK Auger spectra in Co are different in shape and position. The recorded L_2VV CK Auger spectrum in coincidence with the $p_{1/2}$ photoelectrons is located at slightly lower kinetic energies and is narrower compared to the L_3VV Auger spectrum recorded in coincidence with the $p_{3/2}$ photoelectrons. They propose that this is due to the additional hole caused by the CK process increasing the hole–hole interaction energy. This would indicate that the spectrum is not well described by a truly itinerant model. In such a case an additional hole in the valence band would not change the shape of the decay spectrum.

In this paper we present a new APECS study on Cu, Ni and Co performed at the CoESCA station at BESSY II. Our results show consistent behavior with the Cini–Sawatzky model. We also find that the shapes of the L_3VV and the L_2VV CK Auger spectra in Co are very similar, suggesting that these final states are well described within an itinerant model.

2 Experimental methods

In APECS a photoelectron and the corresponding Auger electron originating from the same ionization event are measured simultaneously. Therefore the raw data can be depicted as a 2D map, where every count contains the energy information of the photoelectron and the Auger electron. The raw data consist of both true and accidental coincidence counts where a true count corresponds to a single photoionization event and an accidental count to electrons from different photoionization processes, consequently from two atoms. The accidental counts arrive stochastic at the detector during the correct time window and thus do not represent the true behavior of the system.[20–22] However, the true- to accidental-count ratio is one of the limiting factors of the experiment, since the true count-rate is proportional to the incoming light intensity, I, and the accidental count-rate is proportional to I^2. Thus, in order to keep the accidental to true count-rate low, the incoming light intensity needs to be kept low and subsequently the measurement time becomes long. Data from two consecutive pulses can be used as a measure for the accidental counts,[23] which then can be subtracted from the total data-set resulting in a true coincidence dataset. Partial integration of the true map along the photoelectron kinetic energy or along the Auger electron kinetic energy leads to the Auger electron coincidence spectrum (AECS) or photoelectron coincidence spectrum (PECS), respectively. The main advantage of APECS is the possibility to separate spectral contributions corresponding to different ionization and decay channels. In particular, this means that we can access the corresponding Auger channel to a selected core-ionized state by taking only particular photoelectron energies into account. Consequently, analyzing the Auger spectra we can conclude on the character of the core-ionized state. For more details concerning the APECS technique and the setup used for the presented experiments see Leitner et al.[23]

The data were obtained utilizing the CoESCA end-station at the BESSY II UE-52 PGM beamline.[23] The measurement chamber is equipped with two angular resolving time-of-flight spectrometers (ArTOFs).[24,25] These allow for high transmission and single shot computation and do not require additional timing setup since the spectrometers are synchronized with the X-ray pulses by a trigger provided by the facility.[26,27] The single bunch operation necessary for time of flight detectors was obtained using pulse picking by the resonant excitation method[28] during multi-bunch operation.

We performed APECS experiments on Cu(100), Ni(100) and Co(1000) single crystals. The crystals were cleaned by sequential ion bombardment and annealing cycles. The procedure was repeated until an overview PES spectrum showed only very small traces from residual gases as O, C, S or N and no traces from other contaminants. The main experimental chamber was operated under UHV conditions (10^{-10} mbar).

For Ni only one map was recorded using the $h\nu = 1250$ eV excitation energy. The map covers the whole $L_{2,3}$ photoelectron region and the $L_{2,3}VV$ Auger electron region. Additional information concerning the experiment and analysis performed on Ni is published elsewhere.[19] Due to experimental limitations, in order to enhance the resolution for Cu and Co three separate regions were measured containing the L_3 peak, the L_2 peak and a region in between used for background estimation. The spectra were acquired at $h\nu = 1400$ eV for Cu and at $h\nu = 1150$ eV for Co, more information on data acquisition can be found in the ESI.† The pure data acquisition time for the presented results amounts to multiple 12 hour shifts for each element.

3 Results and discussion

Fig. 1 shows the L_3VV Auger electron spectra of Cu (a), Ni (c) and Co (e) measured in coincidence with the $2p_{3/2}$ photoelectrons as
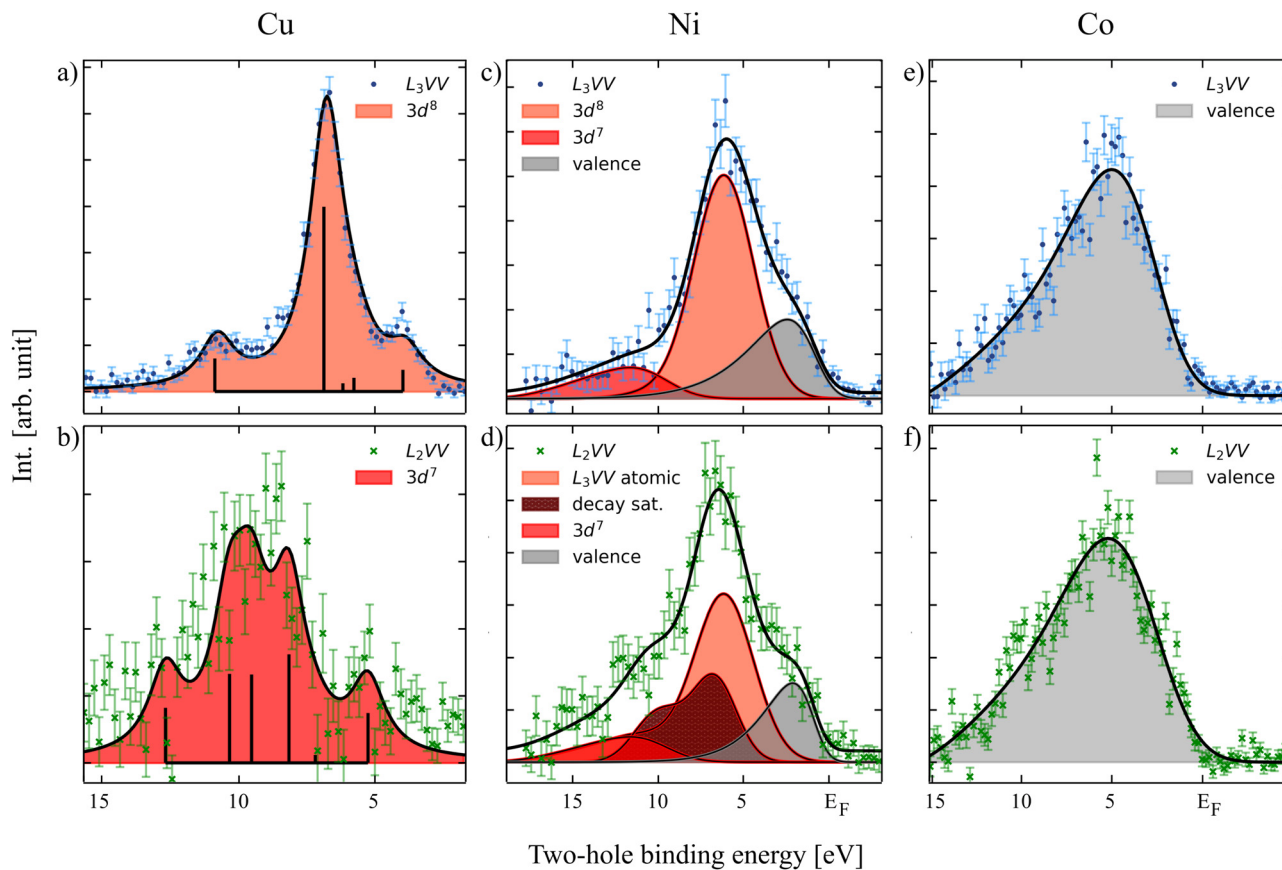
This journal is © the Owner Societies 2022

Phys. Chem. Chem. Phys., 2022, **24**, 19218–19222 | **19219**

Fig. 1 L_3VV (upper panel) and L_2L_3V (lower panel) CK Auger spectra of Cu (a and b), Ni (c and d) and Co (e and f) recorded in coincidence with the $p_{3/2}$ and the $p_{1/2}$ photoelectrons, respectively. The lifetime broadened atomic multiplet contribution to the spectra is shown in different red tones corresponding to different final states. In grey the itinerant part of the spectra is represented by the self-convolution of the valence band photoelectron spectrum.

well as the L_2VV-CK spectra of the same elements (panels b, d and f) measured in coincidence with the $2p_{1/2}$ photoelectrons. The latter spectra are hence due to the decay of a $2p_{3/2}$ hole, but in the presence of an additional hole in the valence shell following the CK decay. The normal L_2VV features, which appear at higher kinetic energies, are not shown. The initial state for the L_3VV Auger decay is a core-hole state for which the energy is accurately known. Therefore, in order to avoid misleading energy scales due to the sample bias used in the experiment, we can plot the Auger spectrum also on a two-hole binding energy scale. In Fig. 1, E_F corresponds to a Auger kinetic energy which is equal to the $2p_{3/2}$ core level binding energy. The L_2VV-CK spectra are plotted on the same energy scale, obtained by subtracting the Auger kinetic energy from the $2p_{3/2}$ binding energy. The data analysis procedure remained the same for all the elements. After the pre-selection of the photoelectron region of interest a Shirley background was subtracted from the resulting coincidence Auger spectra. In case of the L_2VV-CK spectra an additional background contribution was subtracted compensating for the inelastically scattered background originating from the L_3 peak by taking into account the Auger spectrum in coincidence with photoelectrons in the region between the L_2 and the L_3 peaks, discussed in the ESI.†

It is clearly seen that Cu L_3VV and L_2VV-CK show major differences (Fig. 1a and b). This can be explained by the Coster–Kronig (CK) transition, taking place after the excitation of the $2p_{1/2}$ electron, leading to an additional vacancy in the valence compared to the Auger decay after $2p_{3/2}$ electron excitation. Ni shows only minor differences (Fig. 1c and d), which can be seen as an increasing intensity on the low kinetic energy side of the main peak and also on the shape of the high kinetic energy side shoulder. In contrast, Co does not show any differences between the L_3VV and $L_{2,3}VV$-CK decay spectra (Fig. 1e and f).

To explain the behavior we have to take a step back and take a look at the ground state configurations and the possible core-ionized states in these metals. The scheme in Fig. 2 depicts in the left row the possible ground states for Cu, Ni and Co considering the amount of available electrons in the element. In terms of figures, within the configuration interaction model the ground state of solid Cu can be seen as a mixture of $2p^63d^{10}4s^1$ and $2p^63d^94s^2$ states, where the $2p^63d^{10}4s^1$ states are dominant. After photoionization, the screening process that takes place leads to almost exclusively one core-ionized configuration, namely $2p^53d^{10}4s^2$, where the 3d shell is closed. This leads to a very localized electronic structure resembling the atomic behavior of the electrons and holes. Consequently, the
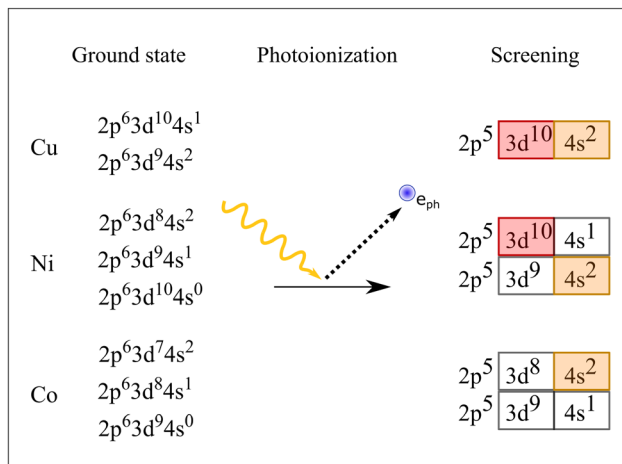
Fig. 2 Photoionization scheme. On the left possible ground state configuration is shown. On the right possible core–hole ionized screened states are depicted. Full 3d shells in the core–hole ionized states are marked in red, full 4s shells in orange. In grey open shells are shown.

L_3VV Auger spectrum can be represented by atomic $3d^8$ multiplet states, as shown by the bars in Fig. 1a. The energy positions of the multiplet levels are taken from Sawatzky.[18] The individual multiplet peaks were represented by Voigt functions where the width and the relative intensities were fit parameters. The best fit was obtained using FWHM of 1.5 eV for all peaks.

For Cu, about 60% of the L_2 holes decay *via* the CK process (see, *e.g.*, the discussion in ref. 29). The CK decay results in $2p^53d^9$ localized states and the following Auger decay leads to $3d^7$ hole states. This leads to a decay spectrum which is very different from the normal L_3VV Auger spectrum.

For Co, on the other hand, we find that the L_3VV spectrum can be represented by the self-convolution of the valence band, here fitted using the valence band spectra recorded by Höchst *et al.*[30] and broadened with a Gaussian. In this case we also find that the L_2VV-CK decay spectrum has the same shape as the L_3VV spectrum. Our results indicate that the width of the two spectra is the same within the error bars. This is in contradiction to previous studies (Lund *et al.*[10]), which indicated that the valence band should become narrower due to the missing CK electron. The initial state for the decay following the CK decay is a $2p_{3/2}$ hole and a 3d valence hole. The fact the two spectra are essentially identical shows that the hole in the valence shell created by the decay becomes delocalized also in the presence of a 2p hole and that the three-hole final state consists of three independent itinerant holes. In this way the valence hole created by the CK decay can be viewed as decoupled from the $2p_{3/2}$ decay and hence that it does not affect the shape of the Auger decay spectrum. This gives further strong support for the interpretation of the Auger spectrum in terms of a truly itinerant model. However, evaluating the results critically one can also suspect small atomic contributions in the Co L_2VV-CK Auger spectrum. An additional peak might be located at about 10 eV two-hole binding energy and also a shoulder might be suspected at around 2 eV. These features

cannot be reproduced by using only the valence band, but taking the error bars into account we do not want to insist on the atomic contribution but mention here that more experimental and theoretical studies are necessary to clarify the true character of Co.

This is different in the case of Ni. The Auger spectrum of Ni is complicated as it contains atomic as well as band-like features. To describe this spectrum it can be helpful to describe the electronic structure of Ni in terms of a mixed-valent situation, see Fig. 2. This is then manifested in a mixed situation also for the screened core-ionized states. These can be $3d^{10}4s^1$ or $3d^94s^2$, leaving the 3d shell closed or open. Thus, the spectrum has to be represented by a mixture of atomic multiplets (shown in red in Fig. 1) and the self-convoluted valence band (in gray). Note that for the sake of clarity we did not show all the possible multiplet energies as in Cu. The values for the $3d^8$ states were calculated by Mårtenson[31] and the multiplet position for the decay satellite was calculated by Sawatzky.[18] As expected the electrons in Ni seem to have a highly correlated nature, leading to pronounced shake-up/off features in the photoelectron and Auger electron spectra. This leads to an additional $3d^7$ contribution in the L_3VV spectrum. The L_2VV-CK spectrum is even more complex. There are many different effects that overlap. Let us discuss the atomic features first. The CK decay in Ni leads to a $3d^9$ intermediate configuration, which as for Cu leads to a $3d^7$ final state after Auger decay (shown in dark red). Note that these $3d^7$ states are different from those produced by shake up in the Auger process and are located closer to the main peak. For a more detailed description of the Ni spectra, see Born *et al.*[19] There were indications that some of these $3d^9$ states delocalize already during the core-hole decay time leading to a $3d^{10}$ core-ionized configuration, producing a replica of the L_3VV Auger spectrum. This will be investigated further.

4 Conclusions

We demonstrated the capabilities of APECS on the transition metal series Cu, Ni and Co and show that from the reconstruction of the coincidence LVV Auger spectra one can deduce information about the itinerancy of the 3d shell and on the character of the screened core-ionized intermediate state after photoionization. As described for Cu, broadened atomic multiplets can be used to fit both the L_3VV and the L_2VV-CK spectra, leading to good agreement between the fit and the data. This can be seen as an indicator for a closed shell configuration in the core-ionized state. For Co, a good fit could be obtained using only the self-convolution of the valence band, demonstrating the itinerant character of the 3d shell, also after core ionization and after creating a double hole in the valence shell. As expected, the Ni spectrum has different overlapping contributions, containing atomic and band-like contributions. Taking both into account a good fit could be obtained confirming the mixed character of the $2p^5$ core-ionized state. However, the spectra show the strongly correlated nature of

This journal is © the Owner Societies 2022

Phys. Chem. Chem. Phys., 2022, **24**, 19218–19222 | **19221**

the electronic structure for Ni. We see in the L_3VV spectrum, that due to a shake-up excitation during the Auger decay localized $3d^7$ states can be produced. As for Cu, also the L_2VV-CK decay leads to $3d^7$ final states. This contribution is, however, shifted, since in this case the initial state for the Auger decay is a $2p^5 3d^9$ core-ionized state. We find that the general trends in the APECS results, when going from Co to Ni and Cu, are well described by the Cini–Sawatzky model.

Conflicts of interest

There are no conflicts to declare.

Acknowledgements

References

1 L. Pietrelli, B. Bellomo, D. Fontana and M. Montereali, *Hydrometallurgy*, 2002, **66**, 135–139.
2 H. Ihara, *Phys. C*, 2001, **364-365**, 289–297.
3 N. T. Z. Potts, T. Sloboda, M. Wächtler, R. A. Wahyuono, V. DAnnibale, B. Dietzek, U. B. Cappel and E. A. Gibson, *J. Chem. Phys.*, 2020, **153**, 184704.
4 V. K. Sikka, J. T. Mavity and K. Anderson, *Mater. Sci. Eng., A*, 1992, **153**, 712–721.
5 M. Hawkins, *Appl. Earth Sci.*, 2001, **110**, 66–70.
6 A. Gonis, N. Kioussis and M. Ciftan, *Electron correlations and material properties*, Springer: New York, NY, 1999.
7 M. Iwan, F. J. Himpsel and D. E. Eastman, *Phys. Rev. Lett.*, 1979, **43**, 1829–1832.
8 N. F. Mott, *Adv. Phys.*, 2006, **13**, 325–413.
9 S. Hüfner, *Photoelectron spectroscopy*, Springer: Berlin, Heidelberg, 2003.
10 C. P. Lund, S. M. Thurgate and A. Wedding, *Phys. Rev. B: Condens. Matter Mater. Phys.*, 1997, **55**, 5455–5465.
11 L. A. Feldkamp and L. C. Davis, *Phys. Rev. B: Condens. Matter Mater. Phys.*, 1980, **22**, 3644–3653.
12 P. A. Bennett, J. C. Fuggle and F. U. Hillebrecht, *Phys. Rev. B: Condens. Matter Mater. Phys.*, 1983, **27**, 2194–2209.
13 M. Cini, *Solid State Commun.*, 1977, **24**, 681–684.
14 M. Cini, *Phys. Rev. B: Condens. Matter Mater. Phys.*, 1978, **17**, 2788–2789.
15 G. A. Sawatzky, *Phys. Rev. Lett.*, 1977, **39**, 504–507.
16 G. A. Sawatzky and A. Lenselink, *Phys. Rev. B: Condens. Matter Mater. Phys.*, 1980, **21**, 1790–1796.
17 H. W. Haak, G. A. Sawatzky and T. D. Thomas, *Phys. Rev. Lett.*, 1978, **41**, 1825–1827.
18 G. A. Sawatzky, *Treatise on Materials Science and Technology*, Academic press, inc., 1988, vol. 30, pp. 167–243.
19 A. Born, T. Leitner, I. Bidermane, R. Ovsyannikov, S. Svensson, N. N. Mårtensson and A. Föhlisch, *Phys. Rev. B*, 2021, **103**, 115121.
20 E. Jensen, R. A. Bartynski, S. L. Hulbert and E. D. Johnson, *Rev. Sci. Instrum.*, 1992, **63**, 3013–3026.
21 J. Lower and E. Weigold, *J. Phys. E: Sci. Instrum.*, 1989, **22**, 421–427.
22 S. Thurgate, B. Todd, B. Lohmann and A. Stelbovics, *Rev. Sci. Instrum.*, 1990, **61**, 3733–3737.
23 T. Leitner, A. Born, I. Bidermane, R. Ovsyannikov, F. Johansson, Y. Sassa, A. Föhlisch, A. Lindblad, F. Schumann and S. Svensson, *et al.*, *J. Electron Spectrosc. Relat. Phenom.*, 2021, **250**, 147075.
24 R. Ovsyannikov, P. Karlsson, M. Lundqvist, L. C. W. Eberhardt, A. Föhlisch, S. Svensson and N. Mårtensson, *J. Electron Spectrosc. Relat. Phenom.*, 2013, **191**, 92–103.
25 D. Kühn, F. Sorgenfrei, E. Giangrisostomi, R. Jay, A. Musazay, R. Ovsyannikov, C. Stråhlman, S. Svensson, N. Mårtensson and A. Föhlisch, *J. Electron Spectrosc. Relat. Phenom.*, 2018, **224**, 45–50.
26 P. S. Kirchmann, L. Retting, D. Nandi, U. Lipowski, M. Wolf and U. Bovensiepen, *Appl. Phys. A: Mater. Sci. Process.*, 2008, **91**, 211–217.
27 A. Oelsner, M. Rohmer, C. Schneider, D. Bayer, G. Schönhense and M. Aeschlimann, *J. Electron Spectrosc. Relat. Phenom.*, 2010, **178-179**, 317–330.
28 K. Holldack, R. Ovsyannikov, P. Kuske, R. Müller, A. Schälicke, M. Scheer, M. Gorgoi, D. Kühn, T. Leitner, S. Svensson, N. Mårtensson and A. Föhlisch, *Nat. Commun.*, 2014, **5**, 4010.
29 R. Nyholm, N. Mårtensson, A. Lebugle and U. Axelsson, *J. Phys. F: Met. Phys.*, 1981, **11**, 1727.
30 H. Höchst, S. Hüfner and A. Goldmann, *Phys. Lett. A*, 1976, **57**, 265–266.
31 N. Mårtensson, R. Nyholm and B. Johansson, *Phys. Rev. B: Condens. Matter Mater. Phys.*, 1984, **30**, 2245–2248.

19222 | *Phys. Chem. Chem. Phys.*, 2022, **24**, 19218–19222

This journal is © the Owner Societies 2022